Inorg. Chem. **1983**, *22*, 3763–3768

Contribution from the Institut de Chimie Minérale et Analytique,
Université de Lausanne, Place du Château 3, CH-1005 Lausanne, Switzerland

Spectroscopic Properties, Electronic Levels, and Crystal Field Parameters of Pentakis(nitrato)europate(III) Ions

J.-C. G. BÜNZLI,* B. KLEIN, G.-O. PRADERVAND, and P. PORCHER[1]

Received March 3, 1983

The structural data of some rare-earth pentanitrates, $X_2Ln(NO_3)_5$, are discussed, and the coordination polyhedra around the metal ion are rationalized by use of different approaches. It occurs that the arrangement of the nitrogen atoms is close to a trigonal bipyramid with D_{3h} symmetry. We have tried to find out whether the spectroscopic properties of $X_2Ln(NO_3)_5$ ($X = Ph_3EtP^+$, Ph_4As^+, and Me_4N^+) reflect this pseudosymmetry, even if the actual site symmetry of the europium ion is C_2 ($X = Ph_3EtP^+$ and Ph_4As^+). IR, Raman, and reflectance spectra are reported and discussed, along with a detailed study of the emission spectra at 77 K. For $(Ph_3EtP)_2Eu(NO_3)_5$, the crystal field splittings indeed display some patterns that can be interpreted as reflecting the higher, pseudotrigonal symmetry. To prove this more quantitatively, the emission spectrum has been simulated by different sets of crystal field parameters by using the method of descending symmetry. With a D_{3h} Hamiltonian, a rms standard deviation of 18 cm^{-1} is obtained; the use of these parameters as starting values for a fit with a C_{2v} Hamiltonian leads to a final, satisfactory, standard deviation of 9.6 cm^{-1}. The coordination polyhedron of $(Ph_4As)_2Eu(NO_3)_5$ seems to be more distorted, since a calculation with a D_{3h} Hamiltonian yields a rather poor fit; a set of C_{2v} parameters reproduces the spectrum with $\sigma = 12$ cm^{-1}. The sets of parameters for the two compounds are rather similar as expected for complexes with similar structure; however, the extreme sensitivity of the emission spectra to the environment of the Eu(III) ion makes it difficult to recognize the pentakis(nitrato) ion solely on the basis of its emission spectrum.

Introduction

Lanthanide nitrates form double salts of different compositions with both inorganic and organic nitrates. All of these salts contain either a hexakis(nitrato) ion[2-4] or a pentakis(nitrato) ion, $Ln(NO_3)_5^{2-}$. In the solid state, hexanitrates are only isolated with the lighter lanthanoid ions, Ln = La–Sm, whereas pentanitrates are isolated for the entire rare-earth series, provided a judicious choice of the counterion is made. A considerable amount of structural work has been performed on pentanitrates, and crystallographic data are available for Ln = La,[5,6], Ce,[7] Sm,[8] Eu,[9] Ho,[10] Er[11], Y,[12] and Sc.[12] In all these species but the last one, the rare-earth ion is surrounded by five bidentate nitrates. For Ln = La and Sm, one or two water molecules are also coordinated to the metal ion, which is therefore 11- or 12-coordinated, whereas the other Ln(III) ions are 10-coordinated. The site symmetry of the metallic ion is low, C_2 or even C_1, which may be the reason why no detailed spectroscopic study of the pentanitrates has been published so far. However, a close examination of the crystal structures reveals that this low symmetry arises sometimes from distortions of a more symmetrical arrangement. Our aim is to test if this latter can be assessed from an analysis of the crystal field splittings. As part of a study of the coordination properties of rare-earth ions, both in solutions[13,14] and in coordination compounds,[15-19] we therefore report the results of a spectroscopic investigation of finely powdered samples of $(Ph_4As)_2Eu(NO_3)_5$, $(Ph_3Et)_2Eu(NO_3)_5$, and $(Me_4N)_2Eu(NO_3)_5$, along with a discussion of their structural properties. The crystal field splittings measured from low-temperature emission spectra (77 K) are reproduced, for the first two compounds, by different sets of crystal field parameters by using the method of the descending symmetry.

Table I. Elemental Analyses of $X_2Eu(NO_3)_5$

	X		
	Ph_4As	Ph_3EtP	Me_4N
% C theor	46.92	45.99	15.75
% C found	46.77	45.87	15.62
% H theor	3.28	3.86	3.96
% H found	3.19	3.86	3.93
% N theor	5.70	6.70	16.07
% N found	5.56	6.77	16.00
% P theor		5.93	
% P found		5.87	
% Eu theor	12.37	14.55	24.83
% Eu found	12.32	14.64	24.72

Experimental Section

Syntheses. The pentakis(nitrato) complexes were prepared by dissolving 5 mmol of Ph_4AsCl (purum, Fluka) or of Ph_3EtBr (purum, Fluka) and adding a solution of 5 mmol of $AgNO_3$ in 25 mL of acetonitrile. The resulting solution was stirred 15 min in the dark and filtered. A solution of 2.5 mmol of $Eu(NO_3)_3{\cdot}6H_2O$ in 15 mL of acetonitrile was added to the previous solution or to 5 mmol of Me_4NNO_3 (puriss, Fluka) in 125 mL of acetonitrile, and the reaction mixture was refluxed for 2–6 h. After partial evaporation of the solvent, a few milliliters of alcohol were added and the complexes crystallized slowly at −15 °C. The microcrystalline, colorless compounds were recrystallized in acetonitrile and dried over phosphorus pentoxide, in vacuo. Satisfactory elemental analyses were obtained

---

(1) Permanent address: Laboratoire des Eléments de Transition dans les Solides, CNRS, Equipe de Recherche No. 210, F-92190 Meudon-Bellevue, France.
(2) Zalkin, A.; Forrester, J. D.; Templeton, D. H. *J. Chem. Phys.* **1963**, *39*, 2881.
(3) Carnall, W. T.; Siegel, S.; Ferraro, J. R.; Tani, B.; Gebert, E. *Inorg. Chem.* **1973**, *12*, 560.
(4) Walker, I. M.; Weeden, H. D. *Inorg. Chem.* **1973**, *12*, 772.
(5) Eriksson, B.; Larsson, L. O.; Niinistö, L.; Valkonen, J. *Inorg. Chem.* **1980**, *19*, 1207.
(6) Eriksson, B.; Larsson, L. O.; Niinistö, L.; Valkonen, J. *Acta Chem. Scand., Ser. A* **1980**, *A34*, 567.
(7) Al Karaghouli, A. R.; Wood, J. S. *J. Chem. Soc., Dalton Trans.* **1973**, 2318.
(8) Burns, J. H. *Inorg. Chem.* **1979**, *18*, 3044.
(9) Bünzli, J.-C. G.; Klein, B.; Chapuis, G.; Schenk, K. J. *J. Inorg. Nucl. Chem.* **1980**, *42*, 1307.
(10) Toogood, G. E.; Chieh, C. *Can. J. Chem.* **1975**, *53*, 831.
(11) Sherry, E. G. *J. Inorg. Nucl. Chem.* **1978**, *40*, 257.
(12) Addison, C. C.; Greenwood, A. J.; Haley, M. J.; Logan, N. *J. Chem. Soc., Chem. Commun.* **1978**, 580.
(13) Bünzli, J.-C. G.; Yersin, J.-R. *Inorg. Chem.* **1979**, *18*, 605.
(14) Bünzli, J.-C. G.; Yersin, J.-R.; Mabillard, C. *Inorg. Chem.* **1982**, *21*, 1471. Bünzli, J.-C.; G.; Mabillard, C.; Yersin, J.-R. *Ibid.* **1982**, *21*, 4214.
(15) Bünzli, J.-C. G.; Klein, B.; Wessner, D. *Inorg. Chim. Acta* **1980**, *44*, L147.
(16) Bünzli, J.-C. G.; Klein, B.; Wessner, D.; Schenk, K. J.; Chapuis, G.; Bombieri, G.; De Paoli, G. *Inorg. Chim. Acta* **1981**, *54*, L43.
(17) Bünzli, J.-C. G.; Klein, B.; Chapuis, G.; Schenk, K. J. *Inorg. Chem.* **1982**, *21*, 808.
(18) Bünzli, J.-C. G.; Klein, B.; Wessner, D.; Alcock, N. W. *Inorg. Chim. Acta* **1982**, *59*, 269.
(19) Bünzli, J.-C. G.; Moret, E.; Yersin, J.-R. *Helv. Chim. Acta* **1978**, *61*, 762.

0020-1669/83/1322-3763$01.50/0

Table II. Eu–O and Nitrate Vibrations of $[Eu(NO_3)_5]^{2-}$ (cm^{-1})

	Ph_4As		Ph_3EtP		Me_4N	
assgnt[a]	IR	R[b]	IR	R	IR	R
Eu–O	176	184	173	190		
Eu–O	211		212	212		
Eu–O	228	232				
Eu–O	238	241				
ν_5		708		705		
ν_3	738	740	738	736	730	738
ν_3	744		746		745	749
ν_6	816		814	820	821	
ν_2	1023	1025	1025	1025	1032	1029
ν_2	1030	1034	1032	1030	1042	1039
ν_4	1311	1314	1313	1316	1305	
ν_1	1452		1460		1460	
ν_1	1479		1482	1481		
ν_1	1488	1495	1491	1496	1490	1515
$\nu_3 + \nu_2$	1730		1732		1735	
$\nu_3 + \nu_2$	1774		1768		1742	
$\nu_3 + \nu_2$					1780	

[a] The nitrate assignments are given in terms of bidentate ions with C_{2v} symmetry. [b] Raman spectra.

for all the complexes and are listed in Table I.

Spectroscopic Measurements. IR spectra were measured as Nujol mulls or KBr pellets by using a Perkin-Elmer 577 spectrometer or a Bruker IFS-113c interferometer. Raman spectra were recorded on a Spex Ramalog-4 spectrometer (647-nm excitation by means of a Spectra-Physics Kr-laser). Reflectance spectra were recorded on a Perkin-Elmer Hitachi spectrometer, Model 340, equipped with a Perkin-Elmer R10-A integrating sphere. The fluorescence spectra were excited either by a Zeiss 450-W xenon high-pressure lamp coupled with a Zeiss M-20 monochromator (band-pass used 4–10 nm) or by a Coherent CR-599 dye laser pumped by a Coherent CR-8 argon laser. The fluorescent light was analyzed at 90° with a 0.5-m Czerny-Turner monochromator from Spex Industries (Model 1870) equipped with a 1200 lines/mm grating blazed at 26° 45′, with a maximum resolution of 0.02 nm. Light intensity was measured by a RCA 31034 photomultiplier with a cooled Ga-As photocathode (dark count 8 ips at 1940 V and −20 °C), coupled to an Ortec photon-counting unit. Low-temperature measurements were performed with an Oxford DN-704 cryostat, and the samples were put into a specially designed rotatable probe to allow for precise alignment. Fluorescent lifetimes were measured by using a flash-lamp-pumped CMX-4 dye laser from Chromatix. The output signal of the photomultiplier was fed to a Bruker BC-104 transient recorder coupled to a DL-4000 signal averager and a DL-450 microprocessor from Datalab.

X-ray powder diffraction diagrams were obtained by using Cu Kα radiation, a Guinier camera, and an Ital-Structure generator. All the data reported in this paper are averages of two to six determinations on at least two independent samples, prepared in the drybox under a nitrogen atmosphere containing less than 10 ppm of water.

Results and Discussion

Vibrational Spectra. The vibrational spectra of the three pentanitrates are closely related and exhibit three kinds of vibrations arising from (i) the lattice and Eu–O vibrations, (ii) the nitrato groups, and (iii) the counterions. The latter could be identified by comparison with reference compounds containing the same cations. In our case, however, they do not provide relevant information about the structural properties of the pentakis(nitrato) ion and are therefore not discussed here. The situation is different for the nitrate vibrations (Table II): the presence of six bands in the IR spectra indicate that these anions are coordinated to the central ion. The weakness of the Raman emission from the $\nu_4(B_1)$ stretching mode, the position of $\nu_1(A_1)$ and $\nu_2(A_1)$ at ca. 1470 and 1030 cm^{-1}, respectively, and the presence of two combination bands separated by more than 20 cm^{-1} in the 1730–1770-cm^{-1} region[20] are all consistent with the presence of bidentate nitrates.

Table III. Fit between Ideal Polyhedra and Crystallographic Data for $X_2Ln(NO_3)_5$[a]

Ln	counterion	EDod (C_{2v})	BCDod (D_2)	BCSAP (D_{4d})
Ce	Ph_3EtP^+	0.120	0.209	0.198
Eu	Ph_4As^+	0.197	0.078	0.143
Ho	NO^+	0.064	0.147	0.199
Er	K^+	0.065	0.173	0.197

[a] Listed numbers represent the normalized standard deviation $\epsilon/\langle M\text{-}L\rangle$.[28]

In addition, the fact that several modes are split into two or more components points to inequivalence of the nitrate groups, as expected from the structural data.

Reflectance Spectra ($X = Ph_4As^+$ and Ph_3EtP^+). In addition to the weak 4f–4f transitions, these spectra contain bands from the phenyl-ring transitions at 26 340 and 27 000 cm^{-1} for Ph_4As^+ and 26 600 and 27 500 cm^{-1} for Ph_3EtP^+ as well as one charge-transfer band at 29 450 cm^{-1}. Taking 1.22 as the optical electronegativity of the Eu(III) ion, corrected for spin pairing and for spin–orbit coupling,[21] the resulting optical electronegativity of the nitrato groups turns out to be 2.35, a value slightly larger than for the acetylacetonate ion, 2.2.[22] The importance of the charge transfer can be estimated from Boudreau's empirical formula,[23] taking 21 290 cm^{-1} as the ionization energy of NO_3^-,[24] 48 600 cm^{-1} as the electron affinity of Eu(III),[25] and 2.48 Å as the mean donor–acceptor distance (=Eu–O distance[9]). The ionic character of the Eu–NO_3^- bond amounts then to 0.53, a value comparable to that found in $Eu(THD)_3$, where THD is the bidentate ligand $C_4H_9COCHCOC_4H_9^-$.[25]

Structural Data. In this section, we only discuss the structure of the pentanitrates in which the Ln(III) ion is 10-coordinated. The structure of such species can usually be rationalized in terms of three polyhedra: the bicapped square antiprism (BCSAP, D_{4d} symmetry), the bicapped dodecahedron (BCDod, D_2), and the 4A,6B-expanded dodecahedron (EDod, C_{2v}).[26] One way to find which polyhedron fits the structure is to compare the angles and the edges with those of the experimentally determined polyhedron. According to this method,[27] the coordination polyhedron for $(Ph_4As)Eu(NO_3)_5$ is best described by a BCSAP.[9] However, in the case of bidentate ligands with small "bites" such as the nitrates, the effective distortion of the experimental polyhedron may be overlooked since the method compares averages of edges and angles that should be equivalent. We have therefore calculated the fit between the X-ray structures and these three ideal polyhedra using Dollase's method, as modified by Drew[28] (Table III). According to these data, the coordination around the metal ion in the pentanitrates with Ln = Ce, Ho, and Er can be described in terms of an expanded dodecahedron, whereas $(Ph_4As)_2Eu(NO_3)_5$ seems to have a more symmetrical coordination polyhedron. A third way of describing the coordination around the metal ion is to refer to Bergman and Cotton's postulate.[29] If the nitrate ions are considered as occupying one coordination site, the resulting polyhedron should be close to the ideal polyhedron for CN = 10/2 = 5, that is a trigonal bipyramid with D_{3h} symmetry. To compare

---

(20) Lever, A. B. P.; Mantovani, E.; Ramaswany, B. S. *Can. J. Chem.* **1971**, *49*, 1957.

(21) Van der Sluis, K. L.; Nugent, L. J. *Phys. Rev.* **1972**, *176*, 86.

(22) Reisfeld, R.; Jørgensen, C. K. In "Inorganic Chemistry Concepts: Lasers and Excited States of Rare Earths"; Springer-Verlag: Berlin, 1977; Vol. 1.

(23) Boudreau, E. A.; Jonassen, H. B.; Theriot, J. L. *J. Am. Chem. Soc.* **1963**, *85*, 2896.

(24) Buchel'nikova, N. S. *Usp. Fiz. Nauk* **1970**, *65*, 351.

(25) Boudreau, E. A.; Chen, W. G. *J. Inorg. Nucl. Chem.* **1977**, *39*, 595.

(26) Drew, M. G. B. *Coord. Chem. Rev.* **1977**, *24*, 179.

(27) Dollase, W. A. *Acta Crystallogr., Sect. A* **1974**, *A30*, 513.

(28) Drew, M. G. B. *Prog. Inorg. Chem.* **1977**, *23*, 67.

(29) Bergman, J. G., Jr.; Cotton, F. A. *Inorg. Chem.* **1966**, *5*, 1208.

Table IV. Comparison between the Positions of the Nitrogen Atoms of $X_2Ln(NO_3)_5$ and the Trigonal Bipyramid[a]

	trig bipyr	Ce[7]	Ho[10]	Er[11]	Eu[9]
α_1, deg	120	119.3	118.5	119.4	117.4
α_2, deg	120	121.5	124.6	120.8	124.3
α_3, deg	120	119.3	116.7	119.7	117.8
β, deg	180	174.6	178.8	179.1	178.1
γ, deg	90	90.0	88.8	88.7	90.0
d(plane), Å		0.00	0.02	0.03	0.00
R(Ln–N), Å[b]		2.972 2.94–3.00	2.870 2.77–2.90	2.856 2.85–2.89	2.896 2.88–2.91

[a] Atoms N_1, N_2, and N_3 are taken as equatorial ligands; their plane should contain the Ln(III) ion. The three angles in this plane are labeled α_i. [b] Mean distance and minimum and maximum bond lengths.

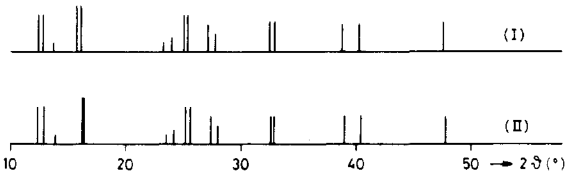

Figure 1. X-ray powder diagrams of $(Ph_3EtP)_2Ln(NO_3)_5$: (I) Ln = Ce; (II) Ln = Eu.

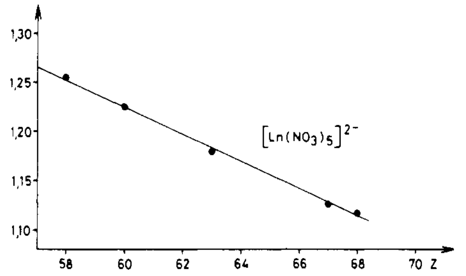

Figure 2. Effective ionic radii of 10-coordinated Ln(III) ions in pentanitrates vs. atomic numbers.

the experimental results with the latter, we have considered the geometrical figure described by the five nitrogen atoms of the nitrate groups (Table IV). The deviations with respect to the ideal polyhedron are particularly small; even the Ln–N distances lie in a narrow range, except for Ln = Ho. As expected for complexes with which the chemical bonds are predominantly ionic, Bergman and Cotton's description is therefore quite precise in the case of the lanthanide pentanitrates. In the next section, we show that this higher D_{3h} symmetry is reflected, for $(Ph_3EtP)Eu(NO_3)_5$, in some features of the crystal field splittings.

Since the crystal structure of $(Ph_3EtP)_2Eu(NO_3)_5$ is not known, we have compared its X-ray powder diagram with that of the corresponding cerium compound. They are almost identical (Figure 1), and therefore, the two pentanitrates can be considered as being isomorphous, so that the Eu(III) ion probably also lies on a site with C_2 symmetry.[7]

Finally, the effective ionic radii of the 10-coordinate Ln(III) ions can be evaluated from the structural data. They are in good agreement with the values obtained from interpolation of ionic radius vs. coordination number plots:[30] r = 1.250 (extrapolated value 1.255), 1.178 (1.180), 1.137 (1.138), 1.120 (1.126), and 1.116 (1.117) Å for Ln = Ce, Eu, Y, Ho, and Er, respectively. These ionic radii seem to decrease linearly with the atomic number Z (Figure 2).

Emission Spectrum of $(Ph_3EtP)_2Eu(NO_3)_5$. The excitation and emission spectra were recorded at 77 K. The excitation spectrum is presented in Figure 3: there is only one sharp, but extremely weak, $^5D_0 \leftarrow {}^7F_0$ transition (full width at half-height, fwhh = 2 Å), consistent with the presence of one crystallographic site for the Eu(III) ion. Selective excitation of this transition with use of a dye laser only produced a Raman spectrum. The emission spectrum is shown on Figure 4; it is dominated by the hypersensitive transition $^5D_0 \rightarrow {}^7F_2$. The integrated and corrected relative intensities of the transitions from the $^5D_0$ level to the ^7F_J manifold are <0.1, 10.3, 100.0, 2.0, 10.4, and 1.6% for J = 0–5, respectively.

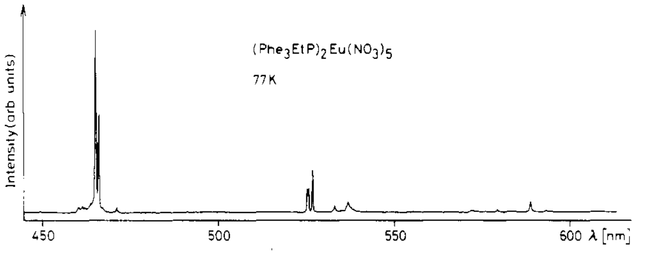

Figure 3. Excitation spectrum of $(Ph_3EtP)_2Eu(NO_3)_5$ at 77 K (analyzing wavelength 618 nm).

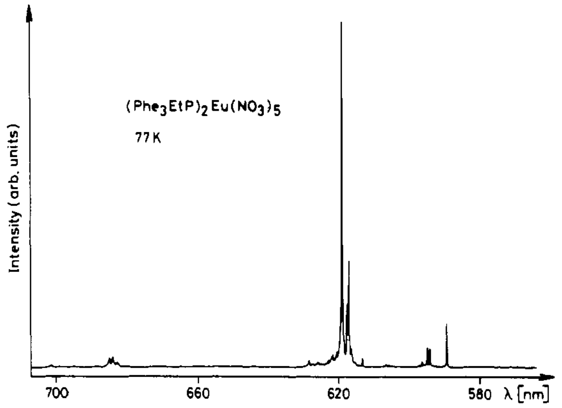

Figure 4. Emission spectrum of $(Ph_3EtP)_2Eu(NO_3)_5$ at 77 K (excitation wavelength 397 nm ($^5L_6$ level)).

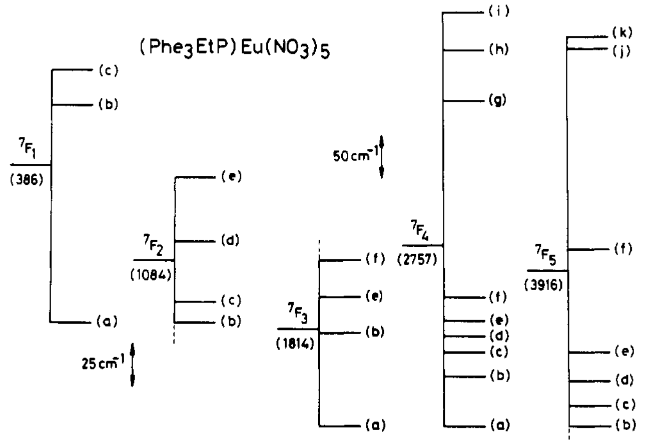

Figure 5. Crystal field splittings of $(Ph_3EtP)_2Eu(NO_3)_5$, in cm^{-1}, from excitation and emission spectra at 77 K. The numbers between parentheses are the barycenters of the levels calculated from the observed transitions.

All the observed transitions in both the excitation and the emission spectra are listed in Tables S1 and S2 (supplementary material), along with their assignment. A scheme of the crystal field splittings for the ^7F_J manifolds is presented in Figure 5. The splitting of the J = 1 and J = 2 level is maximum, which implies a low symmetry. However, a closer look at the crystal field splitting for J = 1 suggests that the sublevels appear as one singlet and one doublet. Moreover, only one main band appears in the emission spectrum for the $^5D_0 \rightarrow {}^7F_2$ transition.

---

(30) Shannon, R. D. *Acta Crystallogr., Sect. A* **1976**, *A32*, 751.

Table V. Calculated Crystal Field Parameters (CFP, cm^{-1}) for $(Ph_3EtP)_2Eu(NO_3)_5$ in D_{3h} and C_{2v} Symmetries

		equiv CFP along C_2 axis		C_{2v} sym	
CFP	D_{3h} sym	sign +	sign −[a]	sign +	sign −[a]
$B^2{}_0$	−276 ± 16	139.4		230 ± 13	192 ± 9
$B^2{}_2$		170.7		173 ± 9	193 ± 7
$B^4{}_0$	−496 ± 24	−186.0		−102 ± 24	−206 ± 23
$B^4{}_2$		−196.0		−246 ± 19	−441 ± 13
$B^4{}_4$		−259.4		−259 ± 15	−102 ± 11
$B^6{}_0$	987 ± 27	−2211	1587	−2190 ± 20	1514 ± 18
$B^6{}_2$		1075	−1704	1072 ± 15	−1739 ± 9
$B^6{}_4$		−855	161	−728 ± 15	24 ± 13
$B^6{}_6$	±1996 ± 16	−407	−521	−636 ± 14	−544 ± 12
σ	18			11.6	9.7

[a] Refers to the $B^6{}_6$ sign in D_{3h} symmetry.

Therefore, it seems that the actual site symmetry is a distortion of a more symmetrical arrangement having a C_{3h} or a D_{3h} symmetry. This latter would indeed correspond to the trigonal-bipyramidal arrangement of the nitrogen atoms of the five nitrate groups (vide supra).

To confirm this, we have tried to reproduce the experimental spectrum by calculating different sets of crystal field parameters (CFP). Despite the high degeneracy of the Eu(III) ion (3003 levels), the 4f^6 configuration is suitable to determine these CFP since the ^7F multiplet is well isolated in the energy level scale: the $^5D_0$ to $^7F_6$ difference amounts to 12 000 cm^{-1}, which implies that the ^7F wave functions are relatively pure in ^7F_J states (>90%). Moreover, the crystal field operator operates only on states with same multiplicity; the ^7F_J multiplet is the only septet of the configuration, and therefore it is reasonable to perform calculations using the reduced base of the 49 $|^7F_{Jm}\rangle$ states.[31] With use of Wybourne's formalism,[32] the crystal field Hamiltonian can be written

$$H_c = \sum_{kqi} B^k{}_q (C^k{}_q)_i \qquad (1)$$

The number of nonzero $B^k{}_q$ CFP depends on the site symmetry. In our case, the low site symmetry, C_2, along with the relatively few experimentally determined levels could lead to difficulties in fitting the spectrum. We have therefore tried to use the descending symmetry principle: D_{3h} was first considered as approximate symmetry in view of the above discussions, allowing us to determine four parameters; these were used as starting parameters to fit the data in the C_{2v} point group of symmetry, which is close to the actual C_2 symmetry.

In the D_{3h} symmetry, the expression for the crystal field Hamiltonian is

$$H_c = B^2{}_0C^2{}_0 + B^4{}_0C^4{}_0 + B^6{}_0C^6{}_0 + B^6{}_6(C^6{}_6 + C^6{}_{-6}) \qquad (2)$$

From the experimental splittings (Figure 5) it is easy to deduce a negative sign for $B^2{}_0$ as well as the magnitude of the $B^4{}_0$ parameter. The accurate determination of the four parameters is done by minimizing the root-mean-square (rms) deviation. The refinement leads to a final standard deviation of 18 cm^{-1} (Table V). The sign of the $B^6{}_6$ parameter cannot be determined since opposite values do not modify the energies but only the labels of the irreducible representations; these latter cannot be obtained from measurements on powders.

The crystal field potential is usually calculated considering the crystallographic axis as the z axis. However, it is possible to express this potential with respect to any other axis. In D_{3h} symmetry, one can therefore express the Hamiltonian (1) with respect to the C_2 axis, which corresponds to the crystallographic axis. It will then be described by nine parameters corresponding to the CFP of the C_{2v} point group of symmetry:

$$H_c(C_{2v}) = B^2{}_0C^2{}_0 + B^2{}_2(C^2{}_2 + C^2{}_{-2}) + B^4{}_0C^4{}_0 + B^4{}_2(C^4{}_2 + C^4{}_{-2}) + B^4{}_4(C^4{}_4 + C^4{}_{-4}) + B^6{}_0C^6{}_0 + B^6{}_2(C^6{}_2 + C^6{}_{-2}) + B^6{}_4(C^6{}_4 + C^6{}_{-4}) + B^6{}_6(C^6{}_6 + C^6{}_{-6}) \qquad (3)$$

These two potentials, $H_c(C_{2v})$ and $H_c(D_{3h})$, are identical, and the relationship between parameters of the same rank is described by a transformation matrix.[33] These parameters are used as starting parameters for the refinement in C_{2v} symmetry. We have determined two sets of parameters because of the uncertainty in the sign of $B^6{}_6$ (Table III). In both cases, the final rms deviations are small but the difference between them does not allow us to decide which is the sign of $B^6{}_6$. In both cases too, the final parameters are not much different from those determined for a D_{3h} symmetry, which means that the adopted procedure of the descending symmetry is valid here. Moreover, the good agreement obtained with the D_{3h} parameters supports the assumption made above on the geometry of the coordination polyhedron, namely that it can be considered as arising from a distortion of a potentially more symmetrical arrangement. It should be stressed here that the more intense component of the $^5D_0 \rightarrow {}^7F_2$ transition corresponds to the allowed transition $A_1' \rightarrow E$ in D_{3h} symmetry. The experimental and calculated levels of the ^7F_J manifold are compared in Table VI.

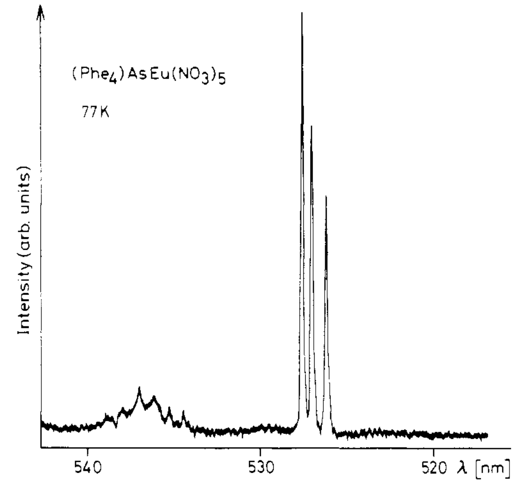

Figure 6. Part of the excitation spectrum of $(Ph_4As)_2Eu(NO_3)_5$ at 77 K (analyzing wavelength 618 nm).

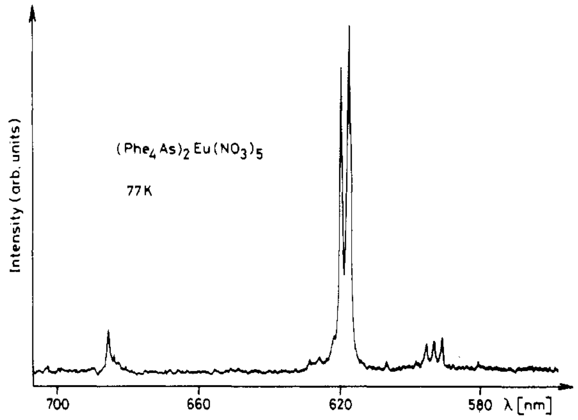

Figure 7. Part of the emission spectrum of $(Ph_4As)_2Eu(NO_3)_5$ at 77 K (excitation wavelength 396 nm).

Emission Spectrum of $(Ph_4As)_2Eu(NO_3)_5$. The excitation and emission spectra were recorded at 77 K. They are partly

---

[31] Porcher, P.; Caro, P. *J. Chem. Phys.* **1981**, *65*, 2108.

[32] Wybourne, B. G. "Spectroscopic Properties of Ions in Crystals"; Wiley-Interscience: New York, 1965.

[33] Porcher, P.; Svoronos, D. R.; Leskelä, M.; Hölsä, J. *J. Solid State Chem.* **1983**, *46*, 101.

Table VI. Comparison between Experimental and Calculated Sublevels for $(Ph_3EtP)_2Eu(NO_3)_5$ (cm^{-1})

		calcd levels					
				C_{2v}			
J	exptl levels	D_{3h}		sign $+^a$		sign $-^a$	
0	0	0	A_1'	0	A_1	0	A_1
1	291	300	A_2'	294	B_2	294	B_2
	422	428	E''	419	B_1	425	B_1
	444	428	E''	442	A_2	437	A_2
2		1023	E''	1016	A_2	1009	B_1
	1046	1023	E''	1030	B_2	1034	A_2
	1059	1069	A_1'	1071	A_1	1063	A_1
	1095	1107	E'	1104	A_1	1104	A_1
	1134	1107	E'	1123	B_1	1135	B_2
3	1696	1700	A_2''	1702	A_2	1701	B_1
	1809	1829	E''	1820	B_1	1813	B_1
		1829	E''	1831	A_2	1834	A_2
		1847	E'	1842	A_1	1837	B_2
	1852	1847	E'	1858	B_2	1860	A_1
	1899	1877	A_1'	1877	B_2	1883	B_2
		2023	A_1''	2022	B_1	2022	A_2
4	2541	2516	A_1''	2516	A_2	2523	B_1
	2601	2620	E'	2594	A_1	2593	A_1
	2629	2620	E'	2632	B_2	2639	A_1
	2650	2635	A_1'	2659	A_1	2655	B_2
	2667	2699	E''	2675	B_1	2678	A_2
	2695	2699	E''	2728	A_2	2721	B_1
	2933	2948	A_2''	2940	B_1	2938	A_2
	2995	3008	E'	2994	A_1	2985	B_2
	3040	3008	E'	3042	B_2	3047	A_1
5		3628	A_2''	3623	A_2	3618	B_1
	3730	3741	E'	3736	B_2	3737	A_1
	3756	3741	E'	3753	A_1	3758	B_2
	3785	3803	E''	3791	A_2	3782	A_2
	3819	3803	E''	3808	A_2	3817	B_1
	3943	3959	A_2'	3952	B_1	3956	B_1
		3969	E''	3977	B_2	3976	B_2
		3969	E''	3987	A_2	3987	A_2
		4183	A_2''	4171	B_1	4175	A_2
	4183	4192	E'	4177	A_1	4181	B_2
	4200	4192	E'	4202	B_2	4205	A_1

[a] Sign of the $B^6{}_6$ parameter (see text).

Table VII. Calculated Crystal Field Parameters (CFP, cm^{-1}) for $(Ph_4As)_2Eu(NO_3)_5$ in C_{2v} Symmetry

CFP	sign $+^a$	sign $-^a$	CFP	sign $+^a$	sign $-^a$
$B^2{}_0$	232 ± 9	326 ± 9	$B^6{}_0$	−2223 ± 24	1481 ± 19
$B^2{}_2$	−26 ± 8	34 ± 5	$B^6{}_2$	973 ± 21	−1560 ± 13
$B^4{}_0$	−352 ± 19	−120 ± 19	$B^6{}_4$	−750 ± 18	+225 ± 16
$B^4{}_2$	−135 ± 18	−345 ± 11	$B^6{}_6$	−437 ± 20	−696 ± 15
$B^4{}_4$	−572 ± 17	−469 ± 13	σ	15.4	12.0

[a] Refers to the two starting parameter sets; cf. Table V.

Table VIII. Comparison between Experimental and Calculated Sublevels for $(Phe_4As)_2Eu(NO_3)_5$ (cm^{-1})

		calcd levels, C_{2v}			
J	exptl levels	sign $+^a$		sign $-^a$	
0	0	0	A_1	0	A_1
1	300	319	B_2	299	B_2
	362	347	B_1	351	B_1
	429	425	A_2	440	A_2
2		930	A_2	931	A_2
	1007	1000	B_1	993	B_1
	1026	1022	B_2	1019	A_1
	1068	1064	A_1	1085	A_1
	1082	1102	A_1	1090	B_2
3	1670	1675	A_2	1672	B_1
	1779	1783	A_2	1781	B_1
	1794	1789	B_1	1794	A_2
	1803	1819	A_1	1806	B_2
	1836	1821	B_2	1841	B_2
	1863	1855	B_2	1843	A_1
	1947	1949	B_1	1955	A_2
4	2535	2513	A_2	2514	B_1
	2568	2557	A_1	2552	A_1
	2582	2575	A_1	2589	A_1
	2601	2600	B_2	2599	B_2
	2636	2635	B_1	2643	B_1
	2653	2682	A_2	2680	A_2
	2908	2922	B_1	2916	A_2
	2932	2950	A_1	2936	B_2
	2994	2975	B_2	2981	A_1
5		3706	A_2	3695	B_1
	3767	3790	B_2	3765	A_1
	3829	3819	A_1	3833	B_1
	3845	3846	A_2	3844	B_1
	3872	3874	B_1	3861	A_2
		4005	A_2	3986	A_2
		4013	B_2	4013	B_2
		4033	B_1	4040	B_1
		4281	B_1	4258	A_2
		4286	A_1	4262	B_2
		4287	B_2	4273	A_1
6	4929	4959	B_2	4952	A_1
		4968	A_2	4954	B_1
	5018	5014	B_1	5017	A_2
		5015	A_1	5026	B_2
	5077	5076	A_1	5075	B_1
	5096	5083	B_1	5096	A_1
		5086	A_2	5106	B_1
	5117	5131	A_1	5109	A_2
	5127	5139	A_2	5116	B_2
	5142	5140	B_2	5153	A_1
	5181	5157	B_1	5174	B_2
		5218	B_2	5201	A_2
	5215	5219	A_1	5211	A_1

[a] Sign of the $B^6{}_6$ parameter (see text).

displayed in Figures 6 and 7, respectively, and all the observed transitions are listed in Tables S3 and S4 (supplementary material) along with their assignments. Assignments for the emission spectrum were confirmed by selective excitations to the $^5D_0$ and to the $^5D_1$ levels, with either a dye laser (around 580 nm) or an argon laser (527 nm). The presence of only one sharp $^5D_0 \rightarrow {}^7F_0$ transition (fwhh = 2.4 Å) is again consistent with one crystallographic site for the Eu(III) ion. The integrated and corrected relative emission intensities of the transitions from the $^5D_0$ level to the ^7F_J manifold are 0.4, 11.4, 100.0, 0.8, 9.5, 0.4, and 0.5% for J = 0–6, respectively. This intensity pattern is quite similar to that found for the previous compound, the main differences lying in the intensities of the transitions to the J = 0 and J = 5 levels, which are much larger in the tetraphenylarsonium complex. A scheme of the crystal field splittings for the ^5D_J and ^7F_J manifolds is presented in Figure 8. Contrary to what was observed for the triphenylethylphosphonium complex, the pattern of these splittings along with the presence of a moderately intense 0–0 transition does not reflect a potentially higher symmetry for the europium site than the crystallographic C_2 symmetry. We have therefore calculated the crystal field parameters in C_{2v} symmetry using the sets determined for $(Phe_3EtP)_2Eu(NO_3)_5$ as starting parameters.[34] A difficulty arose because the $^5D_0 \rightarrow {}^7F_2$ transition, when measured with high resolution under laser excitation, displayed too many components as already observed for other complexes.[18,35] We have considered the two closely spaced multiplets at 616.37 and 616.59 nm and at 617.10, 617.20, and 617.27 nm as representing only one

---

(34) A calculation in D_{3h} symmetry results in a poor fit, with σ = 27 cm^{-1}; the parameters are very similar to those obtained for the triphenylethylphosphonium complex.

(35) Judd, B. R. *Phys. Scr.* **1979**, *21*, 526.

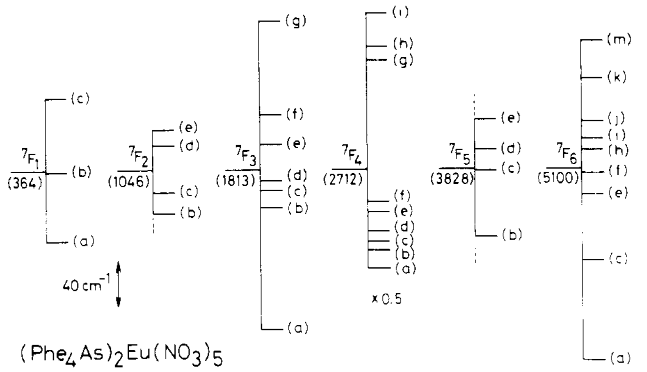

Figure 8. Crystal field splittings of $(Ph_4As)_2Eu(NO_3)_5$, in cm^{-1}, from excitation and emission spectra at 77 K. The vertical scale for $^7F_4$ has been reduced by a factor of 2. The numbers between parentheses are the barycenters of the levels calculated from the observed transitions.

transition. The exact origin of these "additional" splittings is presently under investigation in our laboratory. The results of the spectrum simulation are presented in Tables VII and VIII. Compared to the previous calculation, the overall fit is not as good, although it remains quite acceptable in view of the actual lower symmetry C_2.[36] The set of parameters with a positive $B^6{}_0$ value gives a final standard deviation significantly lower than the other set, and it also better reproduces the splittings of the $J = 1$ and $J = 2$ levels. The corresponding set for the tetraphenylarsonium complex also has a smaller σ and can therefore be considered as more adequate. In general the crystal field parameters for the two pentanitrates have quite similar values, especially the three larger ones, $B^6{}_0$, $B^6{}_2$, and $B^6{}_6$. The only exceptions are $B^2{}_2$ and $B^6{}_4$, which vary by a factor of 8–10 but which are particularly small for Phe_4AsP^+.

Emission Spectrum of $(Me_4N)_2Eu(NO_3)_5$. Depending on the crystallization and drying procedures used, one, two, or even three $^5D_0 \rightarrow {}^7F_0$ transitions are observed for this compound, at 580.2, 579.8, and 579.1 nm, respectively. Perfectly anhydrous samples always display more than one 0–0 transition, while hydrated samples have only one. The crystal field splittings of these latter exhibit a pattern reflecting a higher pseudosymmetry, namely C_{3h} or D_{3h}. We have, however, not analyzed it in view of the uncertainty on the structure of the hydrated compound.

Fluorescence Lifetimes. The fluorescence lifetimes are equal to 0.74 (2) and 0.67 (1) ms for the triphenylethylphosphonium and the tetraphenylarsonium compounds, respectively. They are temperature independent between 77 and 300 K, which means that the nonradiative processes involve a large number of vibrational quanta.[37]

Conclusion

The detailed analysis of the emission spectra and of the structural data of pentakis(nitrato)europate(III) ions performed in this paper allows us to draw some conclusions on the coordination polyhedron around the Eu(III) ion. The bidentate nitrates induce a low symmetry, C_2; however, the nitrogen atoms of these ligands define a more symmetrical arrangement, namely an almost undistorted trigonal bipyramid. For the triphenylethyl compound, the symmetry of this arrangement is reflected in some of the crystal field splittings and the emission spectrum of the Eu(III) ion is reasonably well simulated by a set of four crystal field parameters defining an Hamiltonian in D_{3h} symmetry. This means that in these essentially ionic compounds the Eu(III) ion tends to realize the more compact and more symmetrical arrangement of its ligands. Moreover, the analysis of the crystal field splittings may be used to assess the extent of the distortion of a coordination polyhedron, as indicated by the poorer fit obtained with the tetraphenylarsonium compound, the crystal field splittings of which do not exhibit a pattern reflecting a higher pseudosymmetry. The relative intensity of the forbidden $^5D_0 \rightarrow {}^7F_0$ transition seems to confirm the conclusions drawn from the crystal field splitting analysis: this transition has an extremely low intensity in $(Ph_3EtP)_2Eu(NO_3)_5$, which has the less distorted arrangement, whereas it has appreciably more intensity in the spectra of $(Ph_4As)_2Eu(NO_3)_5$. On the other hand, the extreme sensitivity of the emission spectra to the environment of the Eu(III) ion makes it difficult to recognize the entity $[Eu(NO_3)_5]^{2-}$ solely on the basis of its emission spectrum.

The analysis performed here provides good starting crystal field parameters for a detailed simulation of the emission spectra via the method of descending symmetry. This may be of interest in quantifying the optical properties of potential phosphors for which only powdered samples are available.

Acknowledgment. This research is supported by the Swiss National Science Fondation under Project No. 2.232-0.81. We thank the Fondation Herbette (Lausanne, Switzerland) for the generous gift of the dye and argon lasers. P.P. is grateful to the CNRS (France) for financial support.

Registry No. $(Ph_4As)_2Eu(NO_3)_5$, 76647-81-9; $(Ph_3EtP)_2Eu(NO_3)_5$, 87614-95-7; $(Me_4N)_2Eu(NO_3)_5$, 87614-96-8.

Supplementary Material Available: Excitation spectral data (Tables S1 and S3) and emission spectral data (Tables S2 and S4) (7 pages). Ordering information is given on any current masthead page.

---

[36] One should keep in mind that these CFP were calculated by assuming structural and spectroscopic similarities between the two $[Eu(NO_3)_5]^{2-}$ moieties; it is likely that other CFP sets can be found, which would eventually also yield a good fit of the spectrum.

[37] Auzel, F. *Phys. Rev. B: Solid State* **1976**, *13*, 2809.